

A MASTER EQUATION FOR FORCE DISTRIBUTIONS IN DENSE GRANULAR MATERIALS

Kuniyasu Saitoh¹ and Fumiko Ogushi¹

¹ WPI Advanced Institute for Materials Research, Tohoku University
2-1-1 Katahira, Aoba-ku, Sendai 980-8577, Japan

Key words: granular materials, force-chain network, molecular dynamics simulation

Abstract. Employing molecular dynamics simulations of two-dimensional soft particle packings, we investigate microscopic mechanical responses of granular materials to simple shear deformation. Though microscopic affine responses are deterministic, the restructuring of force-chain networks is well described by a stochastic method for the force distributions, i.e. a master equation. We find that microscopic responses of force-chains are anisotropic in average, while fluctuations of forces are equiprobable in all directions, i.e. the probability of force fluctuations is *isotropic* under simple shear deformation.

1 Introduction

Quasi-static deformations of granular materials have been widely investigated because of their importance in industry and science. However, the macroscopic behavior of dense granular materials is still not fully understood due to disordered configurations and complex dynamics of the constituent particles [1]. At microscopic scale, mechanical responses of granular materials are probed as the change of force-chain networks [2, 3], where complicated non-affine displacements of the particles cause the restructuring of force-chains including opening and closing contacts. If macroscopic quantities, e.g. shear stress, are defined as statistical averages in the force-chains, their mechanical responses to quasi-static deformations are governed by the change of probability distribution function (PDF) of forces. Therefore, the PDFs in dense granular materials have practical importance such that many theoretical studies [4, 5] have been devoted to determine their functional forms observed in experiments [6] and numerical simulations [7].

Recently, we have proposed a master equation for the PDFs as a stochastic description of the restructuring of force-chain networks [8]. The master equation can reproduce the evolution of the PDFs under isotropic (de)compressions, where transition rates or conditional probability distributions (CPDs) in the master equation fully encompass the statistics of microscopic mechanics of dense granular materials.

In this paper, we apply our master equation to the stochastic evolution of force-chain networks under simple shear deformations. First, we explain our numerical method in

Sec. 2. Then, we introduce our theoretical framework in Sec. 3 and show our numerical results in Sec. 4. In Sec. 5, we discuss and conclude our results.

2 Method

We use molecular dynamics (MD) simulations of two-dimensional 50 : 50 binary mixtures of frictionless soft particles with the same mass, m , and two kinds of radii, R and R/ρ ($\rho = 1.4$). The normal force between the particles in contact is given by $f = K\xi - \eta\dot{\xi}$, where K , η , ξ , and $\dot{\xi}$ are a spring constant, viscosity coefficient, particle overlap, and relative speed in the normal direction, respectively [9]. A global damping force, $\mathbf{f}^{\text{damp}} = -\eta\mathbf{v}$, proportional to the particle's velocity, \mathbf{v} , is also introduced to enhance the relaxation, where the damping coefficient, η , is the same with the viscosity coefficient between the particles in contact. Then, we randomly distribute the $N = 8192$ particles in a $L \times L$ square periodic box to make static packings by the method described in Ref. [8], where distances from jamming are defined by the averaged overlaps. In this study, we prepare different 50 packings for each distance from jamming, $\Delta\phi \equiv \phi - \phi_J$, by changing the initial random configurations of the particles, where ϕ and ϕ_J are defined as the area fraction of the particles and the jamming point [3], respectively.

We apply a simple shear deformation to the static packings by replacing every particle positions, (x_i, y_i) , with $(x_i + \Delta\gamma y_i, y_i)$ ($i = 1, \dots, N$), where $\Delta\gamma$ is an infinitesimal strain increment and the Lees-Edwards boundary conditions are used.

3 A Master Equation

Macroscopic mechanical responses of granular materials to simple shear deformations are described by constitutive equations [1]. In this section, we show that constitutive equations can be described by microscopic mechanical responses of force-chain networks through a master equation for the PDFs of forces. In two-dimensional soft particle packings, a microscopic expression of stress tensor is given by $\sigma_{pq} = S^{-1}\langle f_p d_q \rangle$ ($p, q = x, y$), where S , f_p , and d_q are the system area, interparticle force, and relative position (or branch vector) between two particles in contact, respectively. On the right-hand-side, the parentheses, $\langle \dots \rangle$, represent a statistical average over the particles in contacts. In our linear frictionless model, the force is proportional to the overlap and parallel to the relative position. Therefore, introducing a unit vector along the relative position as $(n_x, n_y) = (\cos\theta, \sin\theta)$ with an angle measured from the x -axis (Fig. 1(a)), we can rewrite the force and relative position as $f_p = K\xi n_p$ and $d_q = d(\xi)n_q$, respectively, where $d(\xi) = s - \xi$ is the interparticle distance defined as the difference between the sum of radii, s , and overlap. Then, the stress tensor is rewritten as

$$\sigma_{pq} = \frac{K}{S} \langle \xi d(\xi) n_p n_q \rangle, \quad (1)$$

where the stress tensor is represented by a set of overlap and angle, i.e. $\mathbf{r} \equiv (\xi, \theta)$, which we call *microscopic states* of soft particle packings.

Statistics of the microscopic states are governed by their PDFs, $P_\gamma(\mathbf{r})$, where the subscript, γ , represents the amount of shear strain applied to the system. To introduce the PDFs, we employ the Delaunay triangulations to static packings, where not only the particles in contacts, but also the nearest neighbors without contacts, i.e. the particles in *virtual contacts*, are connected by the Delaunay edges. Then, we generalize “overlaps” as $\xi \equiv s - D$ with the Delaunay edge length, D , where the overlaps between particles in virtual contacts are defined as negative values ($s < D$). Because the total number of the Delaunay edges is conserved during deformations, the PDFs are normalized as

$$\iint P_\gamma(\mathbf{r}) d\mathbf{r} = 1 . \quad (2)$$

When the system is deformed by a small shear strain, $\Delta\gamma$, the microscopic states will change to new states, $\mathbf{r}' \equiv (\xi', \theta')$, as shown in Fig. 1(b), where the new PDF is given by $P_{\gamma+\Delta\gamma}(\mathbf{r}')$. Assuming that the transitions between microscopic states (from \mathbf{r} to \mathbf{r}') are described by the Markov processes, we connect the PDFs before and after simple shear deformation through the Chapman-Kolmogorov equation [10],

$$P_{\gamma+\Delta\gamma}(\mathbf{r}') = \iint W(\mathbf{r}'|\mathbf{r}) P_\gamma(\mathbf{r}) d\mathbf{r} , \quad (3)$$

where $W(\mathbf{r}'|\mathbf{r})$ is the CPD of the microscopic states, \mathbf{r}' , which were \mathbf{r} before the simple shear deformation. By definition, the CPD is normalized as

$$\iint W(\mathbf{r}'|\mathbf{r}) d\mathbf{r}' = 1 . \quad (4)$$

From Eqs. (3) and (4), a master equation for the PDFs is readily obtained as

$$\frac{\partial}{\partial\gamma} P_\gamma(\mathbf{r}') = \iint \{T(\mathbf{r}'|\mathbf{r}) P_\gamma(\mathbf{r}) - T(\mathbf{r}|\mathbf{r}') P_\gamma(\mathbf{r}')\} d\mathbf{r} , \quad (5)$$

where we introduced the transition rate as $T(\mathbf{r}'|\mathbf{r}) \equiv \lim_{\Delta\gamma \rightarrow 0} W(\mathbf{r}'|\mathbf{r})/\Delta\gamma$ [10]. In the master equation (5), the first and second terms in the integral on the right-hand-side represent the gain and loss of new states, \mathbf{r}' , respectively. Therefore, the transition rates or CPDs fully determine the statistics of microscopic responses to shear deformations.

If we take the statistical average, $\langle \dots \rangle$ in Eq. (1), by the PDF, the shear stress defined as $\tau = (\sigma_{xy} + \sigma_{yx})/2$ is given by

$$\tau = \frac{K}{2S} \iint \{\xi d(\xi) \sin 2\theta\} P_\gamma(\xi, \theta) d\xi d\theta , \quad (6)$$

where we used $n_x n_y = \cos \theta \sin \theta = (\sin 2\theta)/2$ and restricted the overlaps to positive values ($\xi > 0$). Then, the shear modulus, $G = \partial\tau/\partial\gamma$, is given by

$$G = \frac{K}{2S} \iint \{\xi d(\xi) \sin 2\theta\} \left\{ \frac{\partial}{\partial\gamma} P_\gamma(\xi, \theta) \right\} d\xi d\theta , \quad (7)$$

which is coupled with the master equation (5) through the derivative of the PDF.

4 Results

4.1 Microscopic responses

To determine the transition rates in the master equation, we first study affine and non-affine responses of microscopic states, $\mathbf{r} = (\xi, \theta)$. When we apply simple shear deformation to the system, the microscopic state will change to $\mathbf{r}_{\text{affine}} \equiv (\xi_{\text{affine}}, \theta_{\text{affine}})$, where each component is given by the initial state as

$$\xi_{\text{affine}} \simeq \xi - \frac{\Delta\gamma}{2} d(\xi) \sin 2\theta, \quad \theta_{\text{affine}} \simeq \theta + \frac{\Delta\gamma}{2} \cos 2\theta, \quad (8)$$

respectively¹. The second term on the right-hand-side of ξ_{affine} represents an anisotropic response of overlaps, where its magnitude becomes maximum in *compressive* and *decompressive* directions, $\theta = \mp\pi/4$, respectively. Note that Eq. (8) is correct for both contacts and virtual contacts. In addition, if we introduce change rates of microscopic states as $\dot{\mathbf{r}}_{\text{affine}} \equiv (\mathbf{r}_{\text{affine}} - \mathbf{r})/\Delta\gamma$, each component is respectively given by

$$\dot{\xi}_{\text{affine}} = -\frac{d(\xi)}{2} \sin 2\theta, \quad \dot{\theta}_{\text{affine}} = \frac{1}{2} \cos 2\theta. \quad (9)$$

In soft particle packings, however, particles are randomly arranged and the force balance between the particles in contacts is broken by simple shear deformation so that particles move around and the system relaxes to a new static state, where the microscopic states change to $\mathbf{r}' = (\xi', \theta')$. Clearly, the microscopic states after relaxation, \mathbf{r}' , as well as their change rates, $\dot{\mathbf{r}} \equiv (\mathbf{r}' - \mathbf{r})/\Delta\gamma \equiv (\dot{\xi}, \dot{\theta})$, are expected to be different from those for affine response, Eqs. (8) and (9). Figures 1(c) and (d) display the angular dependence of change rates, where the affine responses (blue dots) show the deterministic evolution according to Eq. (9), while the non-affine responses (red dots) fluctuate around mean values. In these figures, the mean change rate of overlaps, $\langle \dot{\xi} \rangle$, seems to be quite different from $\dot{\xi}_{\text{affine}}$, while that of angles is almost the same with $\dot{\theta}_{\text{affine}}$, i.e. $\langle \theta' \rangle \simeq \theta_{\text{affine}}$. Therefore, we can write the non-affine microscopic responses as the sum of their mean and fluctuations, i.e.

$$\xi' = f(\xi, \theta) + \psi, \quad \theta' = \theta_{\text{affine}} + \zeta, \quad (10)$$

respectively, where the mean overlap, $\langle \xi \rangle \equiv f(\xi, \theta)$, depends on the initial states and we have introduced *random variables* as ψ and ζ of which standard deviations are given by $v \equiv \sqrt{\langle \psi^2 \rangle}$ and $w \equiv \sqrt{\langle \zeta^2 \rangle}$, respectively. As can be seen in Figs. 1(c) and (d), the standard deviations, v and w , are independent of the initial angle, i.e. they are *isotropic* in space.

¹Eq. (8) is the first-order approximations of an infinitesimal shear strain, $O(\Delta\gamma)$, where the *frame rotation* by simple shear deformation, $\varphi = -\Delta\gamma/2$, has already been subtracted from θ_{affine} and θ' .

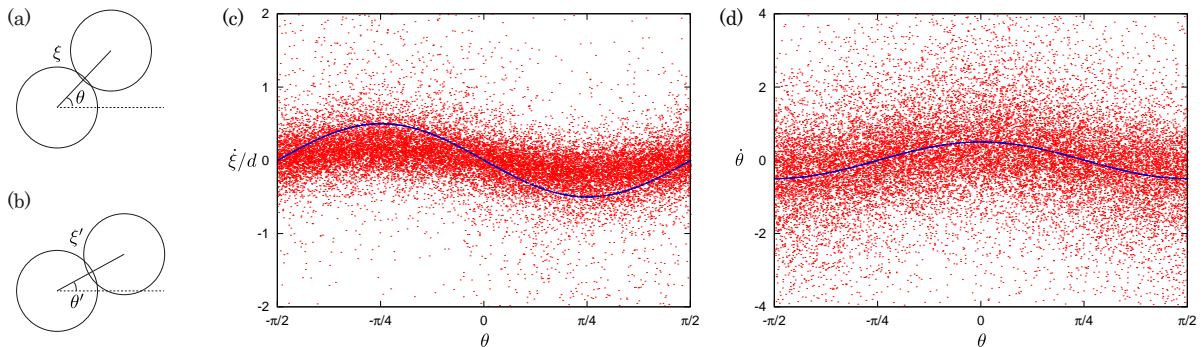


Figure 1: (Color online) Sketches of microscopic states (a) before and (b) after simple shear deformation, $\mathbf{r} = (\xi, \theta)$ and $\mathbf{r}' = (\xi', \theta')$, respectively, where the solid lines connect centers of particles and the dotted lines are parallel to the x -axis. (c) Change rates of overlaps scaled by interparticle distances, $\dot{\xi}/d$, and (d) those of angles, $\dot{\theta}$, plotted against the initial angle, θ , where the blue and red dots are the results of affine and non-affine responses, respectively. The dotted lines in (c) and (d) are $-\sin(2\theta)/2$ and $\cos(2\theta)/2$, respectively. Here, we apply $\Delta\gamma = 10^{-6}$ to the system with $\Delta\phi = 10^{-2}$ (i.e. $\alpha \equiv \Delta\gamma/\Delta\phi = 10^{-4}$).

4.2 Mean and fluctuations

The mean overlap, $f(\xi, \theta)$, can be determined by scattered plots of overlaps before and after simple shear deformation. Figure 2 displays the scattered plots, where we plot the affine and non-affine overlaps after shear, ξ_{affine} (blue dots) and ξ' (red dots), against the initial overlap, ξ . Here, we fixed the initial angle, θ , to compressive (Figs. 2(a) and (b)) or decompressive direction (Figs. 2(c) and (d)). The difference between affine and non-affine responses depends on both the strain step, $\Delta\gamma$, and distance from jamming, $\Delta\phi$, where the difference increases with their ratio, $\alpha \equiv \Delta\gamma/\Delta\phi$. Because overlaps are defined not only between contacts, but also between virtual contacts, there are four kinds of transitions, i.e. *contact-to-contact* ($\xi, \xi' > 0$), *contact-to-virtual* ($\xi > 0, \xi' < 0$), *virtual-to-contact* ($\xi < 0, \xi' > 0$), and *virtual-to-virtual* ($\xi, \xi' < 0$) [8]. In this paper, we restrict our analyses to the first case, contact-to-contact, where both overlaps before and after simple shear deformation remain positive. Then, we introduce the mean overlap for contact-to-contact as a linear fitting function for $\xi' (> 0)$ as

$$f(\xi, \theta) = \{1 + a(\theta)\} \xi + b(\theta) . \quad (11)$$

We also introduce a standard deviation of ξ' around $f(\xi, \theta)$ as v such that systematic deviations from affine responses are quantified by the excess slope, $a(\theta)$, offset, $b(\theta)$, and fluctuation, v , where the affine approximation gives $a(\theta) = (\Delta\gamma/2) \sin 2\theta$, $b(\theta) = -(s\Delta\gamma/2) \sin 2\theta$, and $v = 0$.

Figures 2(e) and (f) display our numerical results of the excess slopes and offsets, where their angular dependence are well captured by sinuous functions,

$$a(\theta) = -A \sin 2\theta , \quad b(\theta) = -B \sin 2\theta , \quad (12)$$

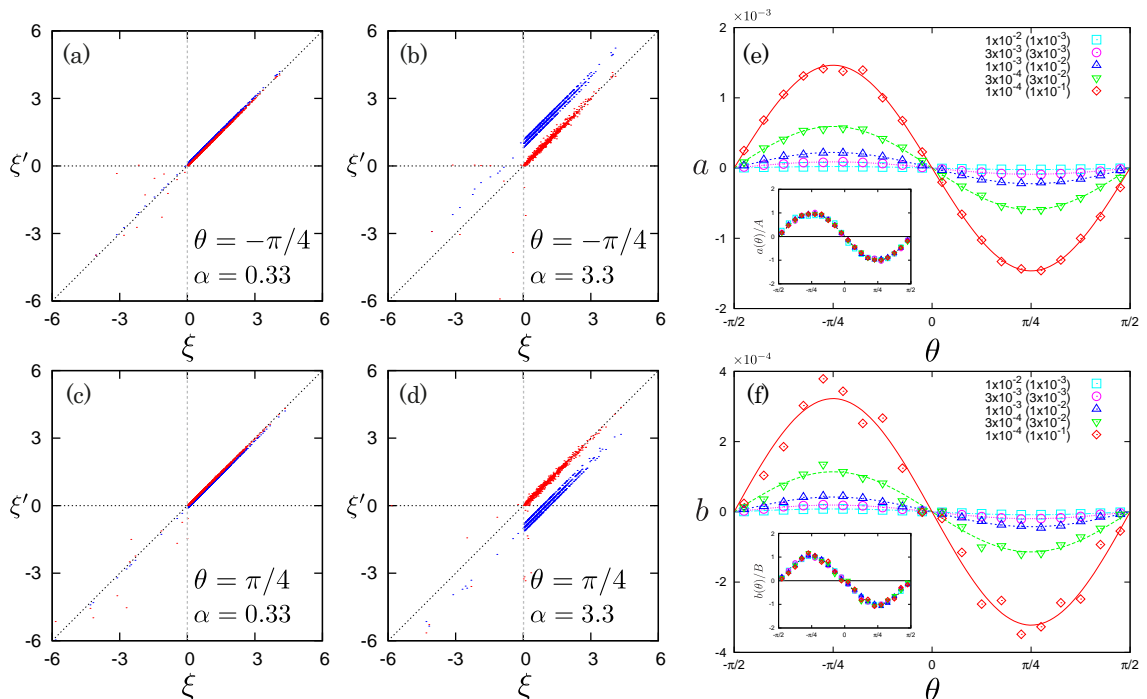


Figure 2: (Color online) Scatter plots of ξ' against ξ scaled by the averaged overlap in the system, where we fix the initial angle to $\theta = -\pi/4$ ((a) and (b)) or $\pi/4$ ((c) and (d)), and change the ratio, α , as shown in the legends. The angular dependence of (e) excess slopes, $a(\theta)$, and (f) offsets, $b(\theta)$, where the lines are fitting functions, (e) $-A \sin 2\theta$ and (f) $-B \sin 2\theta$, respectively. The insets show the data scaled by each amplitude, i.e. $a(\theta)/A$ and $b(\theta)/B$, where the dotted lines represent $-\sin 2\theta$. Here, we apply $\Delta\gamma = 10^{-5}$ to the system with different $\Delta\phi$ (or the ratio, $\alpha \equiv \Delta\gamma/\Delta\phi$) as shown in the legends.

respectively. On the right-hand-side of Eq. (12), the amplitudes, A and B , represent the strength of anisotropic responses of soft particle packings. We have confirmed that the amplitudes, A and B , and fluctuation, v , are increasing functions of the ratio², α . From Eq. (12), the mean overlap, Eq. (11), is rewritten as

$$f(\xi, \theta) = \xi - (A\xi + B) \sin 2\theta, \quad (13)$$

where the sinuous dependence is the same with that of affine response, Eq. (8).

4.3 Conditional probability distributions

The microscopic affine responses are described by the *deterministic* equation (8) so that the CPDs are given by a delta-function, $W(\mathbf{r}'|\mathbf{r}) = \delta(\mathbf{r}' - \mathbf{r}_{\text{affine}})$. However, as shown in Figs. 1 and 2, the microscopic non-affine responses *fluctuate* around their mean values such that the CPDs must have finite widths. In this section, we numerically determine the CPDs by MD simulations.

²Data are not shown. See Ref. [8] for the case of isotropic compressions.

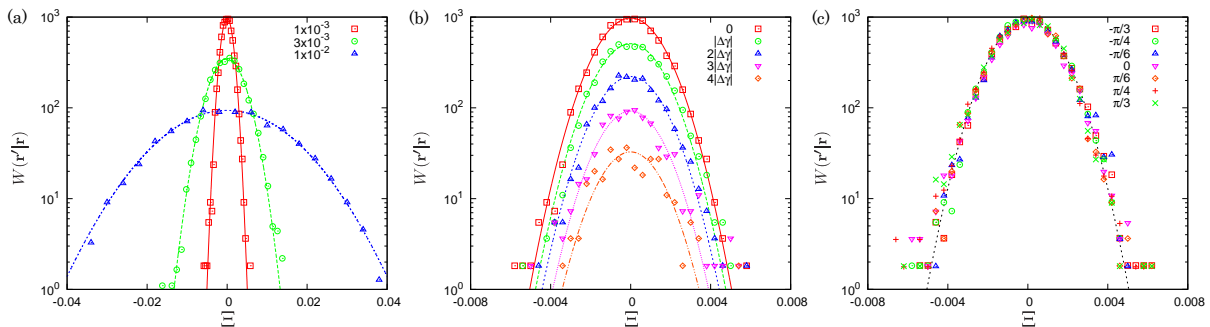


Figure 3: (Color online) CPDs for *contact-to-contact*, $W(\mathbf{r}'|\mathbf{r})$, plotted against the distance from the mean overlap, $\Xi \equiv \xi' - f(\xi, \theta)$, which is scaled by the averaged overlap in the system, where we fixed the initial overlap to $\xi = 1.2$. Different symbols represent different (a) α , (b) $\Delta\theta$, and (c) θ , as shown in the legends, where we used (a) $\theta = -\pi/4$ and $\Delta\theta = 0$, (b) $\alpha = 10^{-3}$ and $\theta = -\pi/4$, and (c) $\alpha = 10^{-3}$ and $\Delta\theta = 0$, respectively. The lines are the Gaussian fitting function, Eq. (14).

Figure 3 displays the CPDs for contact-to-contact, $W(\mathbf{r}'|\mathbf{r})$, plotted against the distance from the mean overlap, $\Xi \equiv \xi' - f(\xi, \theta)$. In Fig. 3(a), we fix the initial angle and angle difference to $\theta = -\pi/4$ and $\Delta\theta \equiv \theta' - \theta_{\text{affine}} = 0$, respectively, while we change the ratio from $\alpha = 10^{-3}$ to 10^{-2} . In Fig. 3(b), the initial angle and ratio are fixed to $\theta = -\pi/4$ and $\alpha = 10^{-3}$, respectively, while the angle difference changes from $|\Delta\theta| = 0$ to $5\Delta\gamma$ (i.e. from $|\dot{\theta}| = 0$ to 5). In Fig. 3(c), the ratio and angle difference are given by $\alpha = 10^{-3}$ and $\Delta\theta = 0$, respectively, but we change the initial angle from $\theta = -\pi/3$ to $\pi/3$. From these results, the CPDs are *symmetric* around the mean value and change their shapes depending on the ratio, α , and angle difference, $\Delta\theta$, while they are independent of the initial angle, i.e. the CPDs are *isotropic* implying that fluctuations of forces are equiprobable in all directions. Therefore, we can decompose the CPDs as

$$W(\mathbf{r}'|\mathbf{r}) = C(\theta'|\theta)Z(\xi'|\mathbf{r}), \quad (14)$$

where $C(\theta'|\theta)$ is another CPD of θ' which was θ before simple shear deformation. Note that $C(\theta'|\theta)$ depends only on the angle difference, $\Delta\theta$, but not on the initial angle, θ , i.e. $C(\theta'|\theta)$ is also *isotropic*, implying that the probability of angle fluctuations is also equiprobable in all directions. The θ' -independent function is given by a Gaussian distribution,

$$Z(\xi'|\mathbf{r}) = \frac{1}{\sqrt{2\pi}v} e^{-\Xi^2/2v^2}, \quad (15)$$

where the lines in Fig. 3 represent Eq. (14) with the Gaussian distribution, Eq. (15).

5 Summary

In this study, we have investigated microscopic mechanical changes of granular materials under simple shear deformations by the master equation and MD simulations. We have found that, though microscopic affine responses are deterministic, microscopic non-affine

responses fluctuate around mean values as a result of complicated non-affine displacements during relaxation. Such the stochastic evolution or restructuring of force-chain networks is well captured by the mean overlap, Eq. (13), and CPD, Eq. (14), where anisotropic mechanical responses of granular materials are well described by the sinuous functions for the excess slope and offset, Eq. (12), and the CPD for contact-to-contact is found to be the isotropic Gaussian distribution function, Eq. (15). Therefore, the fluctuations of overlaps (forces) and angles are equiprobable in all directions even though mechanical responses of granular materials are anisotropic in average.

Acknowledgment

This work was financially supported by World Premier International Research Center Initiative (WPI), MEXT, Japan. A part of numerical computation was carried out at the Yukawa Institute Computer Facility, Kyoto, Japan.

REFERENCES

- [1] J. Lemaitre and J.-L. Chaboche, *Mechanics of Solid Materials* (1990). Cambridge University Press, Cambridge, UK.
- [2] T. S. Majmudar, M. Sperl, S. Luding, and R. P. Behringer, *Phys. Rev. Lett.* (2007) **98**, 058001.
- [3] M. van Hecke, *J. Phys.: Condens. Matter* (2010) **22**, 033101.
- [4] S. Henkes and B. Chakraborty, *Phys. Rev. E* (2009) **79**, 061301.
- [5] J. H. Snoeijer, T. J. H. Vlugt, M. van Hecke, and W. van Saarloos, *Phys. Rev. Lett.* (2004) **92**, 054302.
- [6] E. I. Corwin, H. M. Jaeger, and S. R. Nagel, *Nature* (2005) **435**, 1075.
- [7] L. E. Silbert, G. S. Grest, and J. W. Landry, *Phys. Rev. E* (2002) **66**, 061303.
- [8] K. Saitoh, V. Magnanimo, and S. Luding, *Soft Matter* (2015) **11**, 1253.
- [9] S. Luding, *J. Phys.: Condens. Matter* (2005) **17**, S2623.
- [10] N. G. van Kampen, *Stochastic Processes in Physics and Chemistry*, 3rd edition (2007). Elsevier B. V. Amsterdam, The Netherlands.